Scientific Research Publishing

Optics and Photonics Journal, 2023, 13, 87-96
https://www.scirp.org/journal/opj
ISSN Online: 2160-889X
ISSN Print: 2160-8881

Characteristic Analysis of Off-Axis Meta-Lens

Jingaowa Hu[1,2], Yang Liu[1,2*], Shangnan Zhao[1,2], Lingjie Wang[1], Haokun Ye[1,2], Jianping Zhang[1], Xin Zhang[1,2]

[1]Changchun Institute of Optics, Fine Mechanics and Physics, Chinese Academy of Sciences, Changchun, China
[2]University of Chinese Academy of Sciences, Beijing, China
Email: *hjgw0617@163.com

How to cite this paper: Hu, J.G.W., Liu, Y., Zhao, S.N., Wang, L.J., Ye, H.K., Zhang, J.P. and Zhang, X. (2023) Characteristic Analysis of Off-Axis Meta-Lens. *Optics and Photonics Journal*, **13**, 87-96.
https://doi.org/10.4236/opj.2023.136007

Received: March 14, 2023
Accepted: June 27, 2023
Published: June 30, 2023

Abstract

Meta-lens are a new type of planar optical element that can flexibly manipulate the phase, polarization and amplitude of the beam, and are currently receiving a great deal of attention as they are easier to process and manufacture. Off-axis meta-lens are a special type of meta-lens with a certain degree of dispersion that can be used as a beam-splitting element, providing a unique and feasible way to realize micro-miniature instruments. We analyze the effects of different numerical apertures and off-axis angles on the spectral resolution, focusing efficiency and simulation results of off-axis meta-lens to provide ideas for subsequent research and application of off-axis meta-lens. A number of off-axis meta-lens with parameters NA = 0.408 $\alpha = 13^{\circ}$, NA = 0.18 $\alpha = 13^{\circ}$ and NA = 0.408 $\alpha = 20^{\circ}$ were simulated through Lumerical software. The results show that the off-axis angle is related to the resolution; the larger the angle, the better the spectral resolution but the lower the focusing efficiency; when the numerical aperture is smaller, the smaller the coverage of the phase distribution, which will lead to a larger deviation between simulation and theory. The designer needs to balance the numerical aperture, off-axis angle and other parameters reasonably according to the requirements in order to achieve the desired effect. The findings of this study have important reference values for the theoretical analysis of off-axis meta-lens and the design of parameters in practical applications.

Keywords

Meta-Lens, Off-Axis Meta-Lens, Simulation Analysis

1. Introduction

Meta-lens are planar optical devices composed of two-dimensional meta-materials that can flexibly manipulate the phase, polarization, amplitude and other properties of light to achieve control of the spatial distribution of reflected and

transmitted light fields in a compact form [1], and their planar structural characteristics give them the advantages of simple fabrication and low insertion loss, which have become a current research hot spots.

In order to effectively regulate the electromagnetic wave front, conventional lenses generally achieve phase distribution regulation by modulating the geometry or refractive index of the interface, but due to the restricted dielectric constant and magnetic permeability of natural materials, existing conventional optical lenses are usually large in size and not easily integrated [2]. Meta-lens can obtain the desired phase distribution by adjusting the distribution of the unit structure, which can greatly reduce the size and volume of the element. Depending on the application, different types of meta-lens have been designed, such as achromatic meta-lens [3] [4] [5] [6] [7], meta-lens-based band-pass filters [8], sub-resolution meta-lens [9] [10], artificial intelligence-assisted meta-lens [11], color holography [12] [13] [14], multifunctional meta-lens [15] [16] [17] [18] and re-configurable meta-lens [19] [20] [21].

Off-axis meta-lens has certain dispersion capability compared to co-axial meta-lens, which are intercepted partly off-centre on a co-axis Meta-lens, and the focusing position changes when beams of different wavelengths are incident, which can be achieved by controlling the phase distribution to focus at a specified position. Off-axis meta-lens can be applied in spectrometers, providing new ideas for the realization of compact spectrometers.

In 2016, Khorasaninejad studied a compact spectrometer in the near-infrared band based on off-axis meta-lens, which were designed with off-axis angles of 45˚ and 80˚, respectively. In addition, the working band can be increased by stitching together multiple meta-lens to achieve high resolution over a wide wavelength range [22]. In 2017, Capasso's group also studied a compact spectrometer in the visible band based on off-axis meta-lens with a spectral resolution as small as 0.3 nm and a total working wavelength range of more than 170 nm, and integrated multiple meta-lens with different numerical apertures on a single substrate, making it possible to have a variety of different spectral resolutions and a flexible working wavelength range [23]. In 2018, Yungui Ma's group at Zhejiang University investigated the effect of structural parameters on the effective spectral range and spectral resolution of an off-axis meta-lens-based spectrometer using fluctuating optics and geometrical optics methods. Two off-axis meta-lens-based spectrometers were numerically proposed for different applications [24]. In 2019, the Capasso research team implemented a miniature aberration-corrected spectrometer with nanometer spectral resolution using an off-axis meta-lens, operating at a distance of only a few centimeters from the lens to the detector, a distance that is essentially unconstrained in any way [25].

Currently, research on off-axis meta-lens at home and abroad is limited by a single application scenario and incomplete characterization. More detailed parametric analysis is needed to fully understand the characteristics of off-axis meta-lens, and this information is crucial for the design of micro-compact devices based on off-axis meta-lens. In order to further enhance the influence of

off-axis meta-lens design parameters on its spectral focusing capability, we have carried out simulations of off-axis meta-lens with different parameters, analyzed the effect of off-axis angle on spectral resolution and focusing efficiency, and analyzed the effect of numerical aperture on the deviation of the theoretical calculation results from the simulation results of the focusing position of the meta-lens, in order to provide a reference for the subsequent development of off-axis meta-lens design and extended applications.

2. Working Principle of Off-Axis Meta-Lens

There are three types of meta-lens to achieve phase modulation in the 0 - 2π range: transmission phase type, circuit phase type and geometric phase type [26]. We use transmission phase type meta-lens to achieve phase coverage of 0 - 2π by selecting pillars of different radii.

2.1. Co-Axis Meta-Lens

As shown in **Figure 1(a)**, the focus position of the co-axis meta-lens is on the axis and the phase distribution satisfies Equation (1):

$$\Phi(x,y)=\frac{2\pi}{\lambda}\cdot\left(f-\sqrt{x^2+y^2+f^2}\right) \tag{1}$$

2.2. Off-Axis Meta-Lens

As shown in **Figure 1(b)**, the phase at the origin of the plane where the off-axis meta-lens is located is Φ(0), and the phase at any position on the off-axis meta-lens is Φ(*x*, *y*). The focus position *F* is selected, and if the beam is to be focused at the point *F*, the phase needs to satisfy Equation (2):

$$\Phi(0)+\frac{2\pi}{\lambda}\cdot\sqrt{x_f^2+y_f^2+z_f^2}=\Phi(x,y)+\frac{2\pi}{\lambda}\cdot\sqrt{\left(x-x_f\right)^2+\left(y-y_f\right)^2+z_f^2} \tag{2}$$

According to Equation (2), the phase distribution function of the off-axis meta-lens with focus position (x_f, y_f, z_f) is [23]:

$$\Phi(x,y)=\frac{2\pi}{\lambda}\left[f-\sqrt{\left(x-x_f\right)^2+\left(y-y_f\right)^2+z_f^2}\right] \tag{3}$$

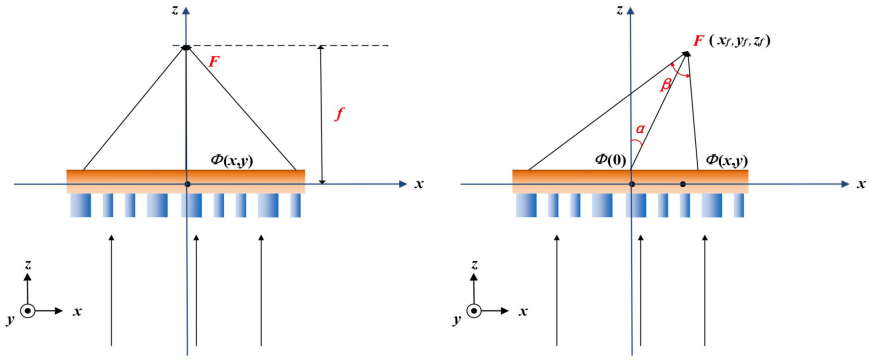

Figure 1. Focusing diagram. (a) Co-axis meta-lens. (b) Off-axis meta-lens.

Off-axis meta-lens can be focused in any position and have some dispersion capability compared to Co-axis meta-lens. Once the focus position has been selected, the discrete phase distribution on the off-axis meta-lens is obtained by Equation (3) to achieve modulation of the incident light wave.

3. Characterization of Off-Axis Meta-Lens

In order to avoid the influence of polarization, a cylindrical cell structure with a height of 1 um and a cell period of 500 nm is chosen, the material of the pillar is Si, and the substrate material is SiO_2. The phase distribution corresponding to different radius unit structures is shown in **Figure 2**.

When performing off-axis meta-lens characterization, the phase distribution can be obtained by Equation (3) after the off-axis focusing angle, NA, has been selected. After selecting a cell structure in the phase library that is close to the desired phase, we use Lumerical to model and simulate an off-axis meta-lens.

1) Effect of different numerical apertures on simulation results

The tensor angle of the off-axis meta-lens at the focus position in **Figure 1** is β. The numerical aperture NA = $\sin(\beta/2)$. When the off-axis meta-lens diameter D and the off-axis angle α are fixed, different NA will result in different ranges of calculated phase distributions. **Figure 3** shows the theoretical phase distribution and Lumerical simulation results for an off-axis meta-lens with D = 30 um, α = 13˚, incident wavelength λ_0 = 1.55 um and focal length f = 32.986 um, where NA = 0.408.

Figure 4 shows the theoretical phase distribution and Lumerical simulation results for an off-axis meta-lens with D = 30 um, α = 13˚, incident wavelength λ_0 = 1.55 um and focal length f = 80 um, where NA = 0.18.

According to **Figure 3(a)** and **Figure 4(a)**, it can be seen that for off-axis meta-lens, when the NA is small, the phase distribution range is reduced, as in **Figure 4(a)** where the right half of the phase is covered. Comparing the deviation of the theoretical calculation and simulation of the focus position for different NA in **Table 1**, it can be seen that the smaller the NA, the larger the deviation

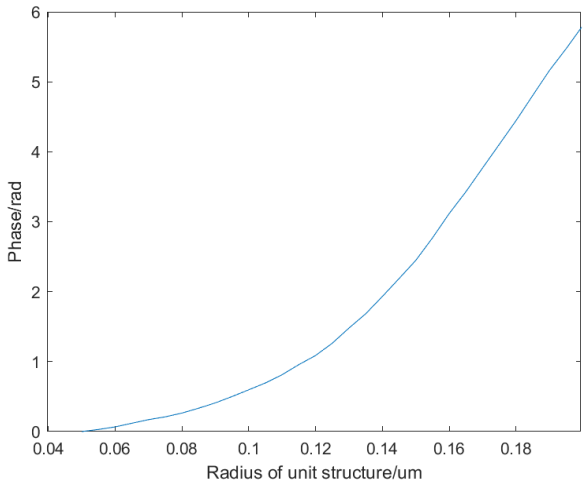

Figure 2. Design flowchart of off-axis meta-lens.

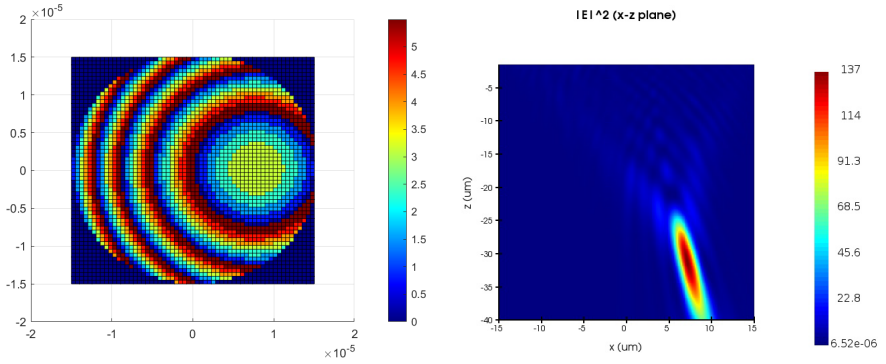

(a) (b)

Figure 3. Phase distribution and simulation results for D = 30 um, $\alpha = 13^{\circ}$, $\lambda_0 = 1.55$ um, $f = 32.986$ um. (a) Phase profile. (b) Simulation result diagram.

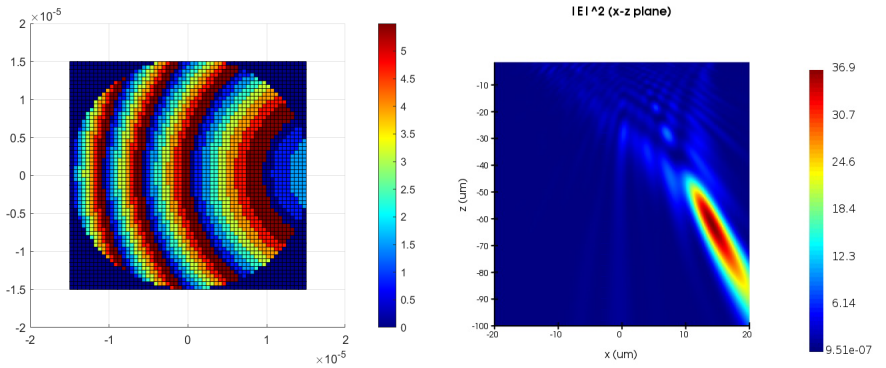

(a) (b)

Figure 4. Phase distribution and simulation results for D = 30 um, $\alpha = 13^{\circ}$, $\lambda_0 = 1.55$ um, $f = 80$ um. (a) Phase profile. (b) Simulation result diagram.

Table 1. Comparison of theoretical calculation and simulation focusing positions of off-axis meta-lens with different NA (Unit: um).

Comparison of Theoretical calculation and simulation focusing positions of off-axis meta-lens with Different NA (Unit: um)				
Parameters	NA	Theoretical focus positions *x*-*z*	Simulation of focus position *x*-*z*	Deviation δx-δz
	0.408	(7.4202, 32.141)	(7.1, 31.2)	(0.3202, 0.941)
	0.18	(17.996, 77.9496)	(14, 62)	(3.996, 15.9496)

between the theoretical calculation and simulation, and the size of the deviation depends on the size of the missing part of the phase.

Therefore, in order to more accurately analyse the effect of different off-axis angles on the resolution and focusing efficiency, and to reduce the deviation of the simulation results from the theory, a meta-lens parameter of NA 0.408 will be chosen for the subsequent analysis.

2) The influence of different off-axis angles on spectral resolution and focusing efficiency

The off-axis meta-lens has a certain dispersion capability, which focuses the beam at different positions when different wavelengths of light are incident. The resolution of the off-axis meta-lens can be calculated from Equation (4) for the corresponding parameters.

$$\begin{aligned}\delta\lambda_{\min} &= \frac{d\lambda}{\left|\Delta\vec{r}\right|}\cdot\frac{0.61\lambda_0}{NA} \\ &= \frac{d\lambda}{f\left\{\sin^{-1}\left[\left(1+\frac{d\lambda}{\lambda_0}\right)\sin\alpha\right]-\alpha\right\}}\cdot\frac{0.61\lambda_0}{\sin\left(\frac{1}{2}\tan^{-1}\frac{4F\cos\alpha}{4F^2-1}\right)}\end{aligned} \tag{4}$$

When NA = 0.408, λ_0 = 1.55 um and D = 30 um, the dispersion characteristics of the off-axis meta-lens were simulated for α = 13˚ and α = 20˚ respectively. As shown in **Figure 5**, the phase coverage of the off-axis meta-lens with different off-axis angles is similar when the NA is the same.

At α = 13˚ and λ_0 = 1.55 um, the minimum resolution of this off-axis meta-lens can be calculated from Equation (4) to be 0.4716 um. As shown in **Figure 6**, comparing the simulation results for λ_0 = 1.55 um and λ_1 = 2.0216 um.

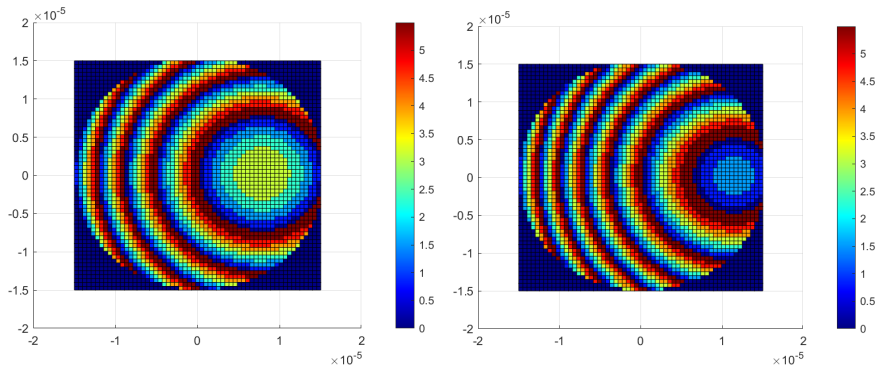

(a) (b)

Figure 5. Phase distribution of off-axis meta-lens with different α. (a) Phase distribution at α = 13˚. (b) Phase distribution at α = 20˚.

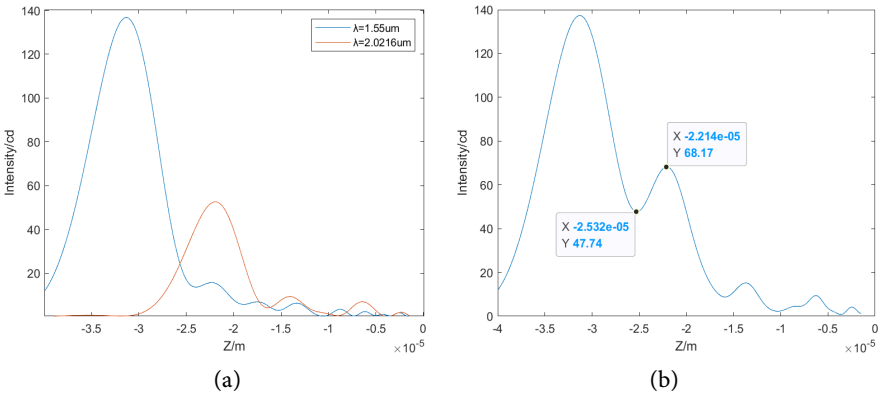

(a) (b)

Figure 6. The intensity distribution of the off-axis meta-lens along the Z axis when α = 13˚ and different λ incident. (a) Z-axis intensity distribution when λ_0 and λ_1 incident. (b) Add the corresponding intensities of the two wavelengths.

According to **Figure 6(b)** it can be seen that the minimal value in the middle of the two maxima is less than 81% of the minimal maxima, which satisfies the Rayleigh criterion, *i.e.* it can be distinguished.

At $\alpha = 20^{\circ}$ and $\lambda_0 = 1.55$ um, the minimum resolution of this off-axis meta-lens can be calculated from Equation (4) to be 0.3063 um. As shown in **Figure 7(a)**, comparing the simulation with $\lambda_0 = 1.55$ um and $\lambda_1 = 1.8563$ um.

According to **Figure 7(b)**, it can be seen that the minimal value in the middle of the two maxima is less than 81% of the minimal maxima, which satisfies the Rayleigh criterion, so that it can be distinguished.

The simulation results show that the larger the off-axis angle, the smaller the spectral resolution when NA is certain.

In addition, for off-axis meta-lens, the choice of off-axis angle has an important influence not only on the spectral resolution, but also on their focusing efficiency. The off-axis meta-lens with a wavelength of 1.55 um and a numerical aperture NA of 0.408 was designed by the control variables method, and off-axis meta-lens with off-axis angles of 13˚, 20˚ and 27˚ were simulated respectively, and the achieved meta-lens focusing efficiency is shown in **Table 2**.

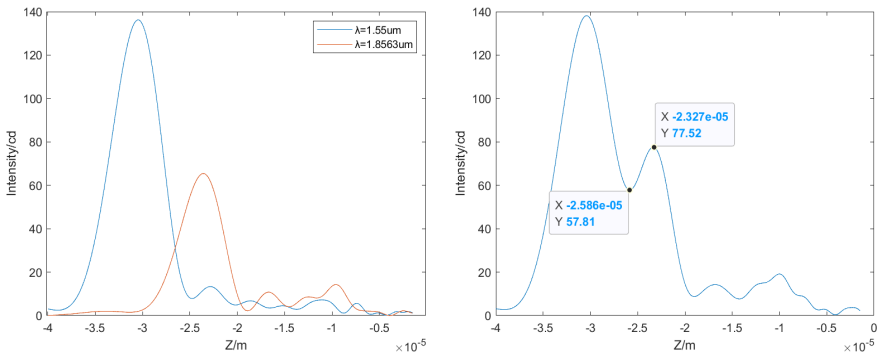

(a) (b)

Figure 7. The intensity distribution of the off-axis meta-lens along the Z axis when $\alpha = 20^{\circ}$ and different λ incident. (a) Z-axis intensity distribution when λ_0 and λ_1 incident. (b) Add the corresponding intensities of the two wavelengths.

Table 2. Simulation results of different parameters (Unit: um).

Comparison of Theoretical calculation and simulation focusing positions of off-axis meta-lens with Different NA (Unit: um)				
Parameters	Off-axis angle α	Working wavelength λ (um)	Spectroscopic resolution (um)	Efficiency in focus
	13˚	1.55	0.4716	59.14%
	13˚	2.0216		29.32%
	20˚	1.55	0.3063	57.36%
	20˚	1.8563		34.86%
	27˚	1.55	0.2263	55.42%

As can be seen from **Table 2**, when NA and incident wavelength are fixed, the focusing efficiency becomes progressively smaller and the spectral resolution gradually increases as the off-axis angle gradually increases. In addition, when NA and off-axis angle α are fixed, if the incident wavelength deviates from the design wavelength, the focusing efficiency will be significantly reduced. If high focusing efficiency and high spectral resolution are to be achieved at the same time, the off-axis angle needs to be chosen as a compromise.

4. Conclusion

This paper presents the working principle of off-axis meta-lens and analyses the effects of different parameters of off-axis meta-lens. The simulation results show that the numerical aperture, off-axis angle and incident wavelength affect the simulation results of off-axis meta-lens. The smaller the numerical aperture, the smaller the coverage of the phase distribution and the larger the deviation between theory and simulation; the larger the off-axis angle, the stronger the dispersion characteristics of the off-axis meta-lens, but the larger the off-axis angle, the lower the focusing efficiency. We will continue our research on the dispersion capability of off-axis meta-lens and design a double-layer diffraction structure based on off-axis meta-lens, which is capable of achieving both color separation and focusing at the same time. This structure can be used in a spectrometer, providing a novel way to achieve an ultra-compact spectrometer.

Acknowledgements

The authors would like to acknowledge the support of The National Natural Science Foundation of China (No. 62005271).

Conflicts of Interest

The authors declare no conflicts of interest regarding the publication of this paper.

References

[1] Xu, B.J., Chen, X.N., Zhao, F., Wang, H.Y. and Du, S.H. (2021) Near-Infrared Wavelength Metalens Design and Simulation. *Laser & Infrared*, **51**, 1466-1471.

[2] Liu, Y.T., Chen, Q.K., Tang, Z.Y., Zhao, Q., Pian, S.J., Liu, X.H., *et al.* (2021) Research Progress of Aberration Analysis and Imaging Technology Based on Metalens. *Chinese Optics*, **14**, 831-850.

[3] Wang, Y., Chen, Q., Yang, W., Ji, Z., Jin, L., Ma, X., *et al.* (2021). High-Efficiency Broadband Achromatic Metalens for Near-IR Biological Imaging Window. *Nature Communications*, **12**, 5560. https://doi.org/10.1038/s41467-021-25797-9

[4] Lin, P., Lin, Y.S., Lin, J. and Yang, B.R. (2021) Stretchable Metalens with Tunable Focal Length and Achromatic Characteristics. *Results in Physics*, **31**, Article 105005. https://doi.org/10.1016/j.rinp.2021.105005

[5] Shan, D., Xu, N., Gao, J., Song, N., Liu, H., Tang, Y., *et al.* (2022) Design of the All-Silicon Long-Wavelength Infrared Achromatic Metalens Based on Deep Silicon

Etching. *Optics Express*, **30**, 13616-13629. https://doi.org/10.1364/OE.449870

[6] Lin, R.Y., Wu, Y.F., Fu, B.Y., Wang, S.M., Wang, Z.H.L. and Zhu, S.H.N. (2021) Application of Chromatic Aberration Control of Metalens. *Chinese Optics*, **14**, 764-781. https://doi.org/10.37188/CO.2021-0096

[7] Li, M., Li, S., Chin, L.K., Yu, Y., Tsai, D.P. and Chen, R. (2020) Dual-Layer Achromatic Metalens Design with an Effective Abbe Number. *Optics Express*, **28**, 26041-26055. https://doi.org/10.1364/OE.402478

[8] Shan, D., Gao, J., Xu, N., Liu, H., Song, N., Sun, Q., *et al.* (2022) Bandpass Filter Integrated Metalens Based on Electromagnetically Induced Transparency. *Nanomaterials*, **12**, 2282. https://doi.org/10.3390/nano12132282

[9] Zuo, R., Liu, W., Cheng, H., Chen, S. and Tian, J. (2018) Breaking the Diffraction Limit with Radially Polarized Light Based on Dielectric Metalenses. *Advanced Optical Materials*, **6**, Article 1800795. https://doi.org/10.1002/adom.201800795

[10] Li, Y., Cao, L., Wen, Z., Qin, C., Yang, J., Zhang, Z., *et al.* (2019) Broadband Quarter-Wave Birefringent Meta-Mirrors for Generating Sub-Diffraction Vector Fields. *Optics Letters*, **44**, 110-113. https://doi.org/10.1364/OL.44.000110

[11] Phan, T., Sell, D., Wang, E.W., Doshay, S., Edee, K., Yang, J. and Fan, J.A. (2019) High-Efficiency, Large-Area, Topology-Optimized Metasurfaces. *Light*: *Science & Applications*, **8**, 48. https://doi.org/10.1038/s41377-019-0159-5

[12] Li, R., Guo, Z., Wang, W., Zhang, J., Zhou, K., Liu, J., *et al.* (2015) Arbitrary Focusing Lens by Holographic Metasurface. *Photonics Research*, **3**, 252-255. https://doi.org/10.1364/PRJ.3.000252

[13] Sajedian, I., Lee, H. and Rho, J. (2019) Double-Deep Q-Learning to Increase the Efficiency of Metasurface Holograms. *Scientific Reports*, **9**, Article 10899. https://doi.org/10.1038/s41598-019-47154-z

[14] Rao, F., Zile, L. and Guoxing, Z. (2021) Research Development of Amplitude-Modulated Metasurfaces and Their Functional Devices. *Chinese Optics*, **14**, 886-899. https://doi.org/10.37188/CO.2021-0017

[15] Avayu, O., Almeida, E., Prior, Y. and Ellenbogen, T. (2017) Composite Functional Metasurfaces for Multispectral Achromatic Optics. *Nature Communications*, **8**, Article 14992. https://doi.org/10.1038/ncomms14992

[16] Jin, J., Pu, M., Wang, Y., Li, X., Ma, X., Luo, J.,*et al.* (2017) Multi-Channel Vortex Beam Generation by Simultaneous Amplitude and Phase Modulation with Two-Dimensional Metamaterial. *Advanced Materials Technologies*, **2**, Article 1600201. https://doi.org/10.1002/admt.201600201

[17] Wei, Q., Huang, L., Li, X., Liu, J. and Wang, Y. (2017) Broadband Multiplane Holography Based on Plasmonic Metasurface. *Advanced Optical Materials*, **5**, Article 1700434. https://doi.org/10.1002/adom.201700434

[18] Cheng, H., Wei, X., Yu, P., Li, Z., Liu, Z., Li, J.,*et al.* (2017) Integrating Polarization Conversion and Nearly Perfect Absorption with Multifunctional Metasurfaces. *Applied Physics Letters*, **110**, Article 171903. https://doi.org/10.1063/1.4982240

[19] Bai, W., Yang, P., Wang, S., Huang, J., Chen, D., Zhang, Z., *et al.* (2019) Actively Tunable Metalens Array Based on Patterned Phase Change Materials. *Applied Sciences*, **9**, 4927. https://doi.org/10.3390/app9224927

[20] Yu, P., Li, J., Zhang, S., Jin, Z., Schütz, G., Qiu, C. W., *et al.* (2018) Dynamic Janus Metasurfaces in the Visible Spectral Region. *Nano Letters*, **18**, 4584-4589. https://doi.org/10.1021/acs.nanolett.8b01848

[21] She, A., Zhang, S., Shian, S., Clarke, D.R. and Capasso, F. (2018) Adaptive Meta-

lenses with Simultaneous Electrical Control of Focal Length, Astigmatism, and Shift. *Science advances*, **4**, eaap9957. https://doi.org/10.1126/sciadv.aap9957

[22] Khorasaninejad, M., Chen, W.T., Oh, J. and Capasso, F. (2016) Super-Dispersive Off-Axis Meta-Lens for Compact High Resolution Spectroscopy. *Nano Letters*, **16**, 3732-3737. https://doi.org/10.1021/acs.nanolett.6b01097

[23] Zhu, A.Y., Chen, W.T., Khorasaninejad, M., Oh, J., Zaidi, A., Mishra, I., *et al.* (2017) Ultra-Compact Visible Chiral Spectrometer with Meta-Lens. *Apl Photonics*, **2**, Article 036103. https://doi.org/10.1063/1.4974259

[24] Zhou, Y., Chen, R. and Ma, Y. (2018) Characteristic Analysis of Compact Spectrometer Based on Off-Axis Meta-Lens. *Applied Sciences*, **8**, 321. https://doi.org/10.3390/app8030321

[25] Zhu, A.Y., Chen, W.T., Sisler, J., Yousef, K.M., Lee, E., Huang, Y.W., *et al.* (2019) Compact Aberration-Corrected Spectrometers in the Visible Using Dispersion-Tailored Metasurfaces. *Advanced Optical Materials*, **7**, Article 1801144. https://doi.org/10.1002/adom.201801144

[26] Luo, X.G. (2017) Sub-Wavelength Electromagnetism. Vol. 1, Science Press, 208-214.